OPTICAL FLOW ROBUST ESTIMATION IN A HYBRID MULTI-RESOLUTION MRF FRAMEWORK

C. Cassisa[1,2] *V. Prinet*[2,3] *L. Shao*[1] *S. Simoens*[1] *C.L. Liu*[2,3]

[1] Lab. of Fluid Mechanics and Acoustics (LMFA)
Ecole Central of Lyon (ECL), France
{cassisa,prinet}@liama.ia.ac.cn

[2] Sino-French Lab. in Information (LIAMA)
[3] National Lab. of Pattern Recognition (NLPR)
Institute of Automation of CAS (CASIA), China.

ABSTRACT

We propose in this paper a robust multi-resolution technique to estimate dense velocity field from image sequences. It couples a Gaussian pyramidal down-sampling decomposition together with a multi-grid approach. At each pyramid level, bilinear interpolation and efficient warping techniques are performed to generate a residual images. The displacement field is computed in a Markov Random Field (MRF) framework. We compare two different methods to minimize the Gibbs energy: a modified Iterative Conditional Mode (ICM) and a Graph-Cut algorithm extended to multi-grid scheme. We validate and demonstrate the robustness of our approach on synthetic and real images for fluid experiment applications.

Index Terms— Motion measurement, Fluid flow, Multi-resolution, Optimization methods.

1. INTRODUCTION

Motion estimation has received a great deal of attention since the early days of computer vision, with applications in video tracking, structure from motion, fluid analysis, ... Though much progress have been done since the first proposed techniques, some fundamental problems are still open.

Differential Optical Flow (DOF) computation, introduced by [1], has proved to be very powerful for motion estimation. The OF equation is based on the hypothesis of illumination constancy over two consecutive frames. Differential OF assumes moreover that the displacement of the object or particle of interest is rather small. These are very restrictive constraints, satisfied by only a small number of movement classes. In [2], Barron *et al.* made a survey of different classical methods for OF computation.

To cope with large displacements, multi-resolution techniques have been proposed. The general idea consists in estimating the OF at different resolutions from coarse to fine, in an iterative and incremental way. The generation of images of different resolutions can be achieved using gaussian pyramid [3], steerable pyramid [4] or more recently wavelet decomposition [5]. Alternatives to solve the same problem are multi-grid or scale-space approaches [6, 7, 8]: the processing parameter (grid size or filter coefficient) varies, while the image resolution is fixed. In addition, Memin [9] and Ruhnau [10] have shown that coupling techniques can improve the accuracy of the estimation. For specific applications, the brightness constancy is withdrawn in favor of grey-level gradient constancy ([11]).

Computational issues regarding the search for the optimal global solution of the velocity field is probably the main focus of attention these last years. Greedy [3, 2], variational [10, 9], or graph-based [12] approaches are evenly used. However, most of these techniques can only converge to a local solution. They are then very sensitive to initialization.

In this paper, we present an efficient formulation and computational framework to estimate accurate motion between two frames. The DOF equation is solved by maximizing a posterior probability. We propose a new hybrid multi-resolution multi-grid (MM) approach, making possible the computation of large displacements while improving significantly the computation time. We compare two optimization techniques: an adapted Graph-Cut algorithm converging to a global solution and a revised Iterative Conditional Mode (ICM) –*i.e.* local search method.

The rest of the paper is organized as follows. Section 2 introduces the essentials of optical flow and its multi-resolution formulation. In section 3, we detail the optimization procedure. Results from synthetic and read data are illustrated and discussed in section 4. We conclude in Section 5.

2. DESCRIPTION OF THE DOF+MM APPROACH

2.1. Problem statement

The velocity field $\mathbf{v}$ is computed within an MRF framework via Maximum a Posteriori estimation. Using a Bayesian decomposition, the total Gibbs energy E is defined by:

$$E(\mathbf{v}, I) = \sum_{s \in C_1} V_d(I_s, \mathbf{v}_s) + \sum_{s,s' \in C_2} \alpha_p V_p(\mathbf{v}_s, \mathbf{v}_{s'}) \qquad (1)$$

This work is partially supported by the sino-french PRA project (SI 05-03).

Algorithm 1 DOF+MM algorithm

Pyramid creation from level 0 (Original) to K (coarsest)
Multi-Resolution Scheme
for $k = K$ to 0 **do**
  if $k \neq K$ *Consider estimated velocity at coarser level* **then**
    $\tilde{\mathbf{v}}^{k+1} = Int(\mathbf{v}^{k+1})$. *Interpolation of* $\mathbf{v}$ *from* $k+1$ *to* k
    $\widetilde{I}_2^k = Warp(I_2^k, \tilde{\mathbf{v}}^{k+1})$. *Warp Image 2 by* $\tilde{\mathbf{v}}^{k+1}$
  else
    $\widetilde{I}_2^k = I_2^k$ *Coarsest level of the pyramid: No warping*
  end if
  Compute Gradient : $\nabla\widetilde{I}_2^k$, $\widetilde{I}_t^k$ *on image* I_2
  Two Steps Multi-Grid
    Compute Gradient Grid : $\overline{\nabla\widetilde{I}}_2^k$, $\overline{\widetilde{I}}_t^k$
    Estimate $d\mathbf{v}_g^{k*}$ *By ICM or Graph Cut*
    Estimate $d\mathbf{v}_l^{k*}$ *By ICM or Graph Cut*
  End Two Step Multi-Grid
    Update $\mathbf{v}^{k*} += \tilde{\mathbf{v}}^{k+1} + d\mathbf{v}^{k*}$
end for
return The dense displacement field: $\mathbf{v}^{0*}$
End Multi-Resolution

where I is the observed data. V_d and V_p are respectively the data potential (or likelihood term) and prior potential (or regularization term); s is a site; C_1 and C_2 are respectively the single-site and pair-site cliques, and α_p is a weighting coefficient.

The data potential is given by the illumination constancy constraint in its differential formulation [1]:

$$V_d(I_s, \mathbf{v}_s) = \left(\nabla I_2(s, t+1).\mathbf{v}_s + I_t(s,t)\right)^2 \qquad (2)$$

where I_1 and I_2 are two consecutive frames at time t and $t+1$; $\nabla I_2(s, t+1)$ and $I_t(s,t) = I_2(s,t+1) - I_1(s,t)$ are the spatial and temporal gradients respectively.

The regularization term is given by:

$$V_p(\mathbf{v}_s, \mathbf{v}_{s'}) = \alpha_p(s)\ ||\mathbf{v}_s - \mathbf{v}_{s'}|| \qquad (3)$$

where $\alpha_p(s)$ is a weighting function of I for each site s; $||.||$ is the L2 or L1 norm.

The searched displacement field between image I_1 and I_2 is given by the optimal configuration $\mathbf{v}^*$ that minimizes E.

2.2. Multi-resolution formulation

Because the direct integration of (2) into (1) does not enable to retrieve large displacements, we derive a multi-resolution pyramidal scheme. The images at multi-levels I^k are computed with a gaussian pyramid [13].

At the lowest resolution K, the velocity field $(\mathbf{v}^K)^*$ is retrieved by minimizing (1), using (2) and (3), from images I_1^K and I_2^K. At level $k < K$, the image I_2^k is wrapped into an image $\widetilde{I}_2^k$ by the following transformation:

$$\widetilde{I}_2^k(s, t+1) = I_2^k(s - \tilde{\mathbf{v}}^{k+1}, t+1) \qquad (4)$$

where $\tilde{\mathbf{v}}^{k+1}$ is the interpolated velocity estimated from $\mathbf{v}^{k+1}$. The data potential at level k now writes:

$$V_d^k(I_s^k, v_s^k) = \left(\nabla\widetilde{I}_2^k.\, d\mathbf{v}_s^k + \widetilde{I}_t^k\right)^2 \qquad (5)$$

where $\nabla\widetilde{I}_2^k$ is the spatial gradient of $\widetilde{I}_2^k$ and $\widetilde{I}_t^k = \widetilde{I}_2^k - I_1^k$. $d\mathbf{v}^k$ is the differential velocity vector computed at level k. Thus, at each level k of the pyramid, the velocity field is given by: $\mathbf{v}^k = \tilde{\mathbf{v}}^{(k+1)} + d\mathbf{v}^{k*}$, with $0 \leq k < K$ and $\tilde{\mathbf{v}}^K \leftarrow (\mathbf{v}^K)^*$.

2.3. Multi-grid computation

In order to speed up the computation, we make use of a coarse to fine (or multi-grid) approach originally proposed in [14]. At each level of the Gaussian pyramid, the velocity $d\mathbf{v}$ is decomposed into a global component $d\mathbf{v}_g$ –average over a mesh size— and a local component $d\mathbf{v}_l$ –local deviation from $d\mathbf{v}_g$. $d\mathbf{v}_g$ is, per construction, very fast to compute, and furnishes a very good approximation of the final displacement.

3. OPTIMIZATION

At each pyramid level $k < K$, we search for the optimal $d\mathbf{v}^*$ that minimizes (1) using (3) and (5). At first, $d\mathbf{v}_g^*$ is computed over grid cells, considering that $d\mathbf{v} = d\mathbf{v}_g$ ($d\mathbf{v}_l = 0$). $d\mathbf{v}_g^*$ is then duplicated or interpolated at each pixel. Secondly, $d\mathbf{v}_l^*$ is estimated, while keeping $d\mathbf{v}_g$ constant. We compare two different minimization methods: an extended ICM and an adapted Graph-Cut.

Iterative Conditional Modes Using ICM [15], we introduce an iteration-dependent weighting function: $\alpha_p(s) \rightarrow \alpha_p(s,i)$, where i counts for the iteration number and $\alpha_p(s,i)$ is increasing with i. The energy decrease is mainly data-driven at the beginning of the iterations, and it is only when the energy is close to stabilization that the regularization term is reinforced. By this way, the convergence is fast and robust, with a final configuration which is properly smoothed.

Graph Cuts In the α-expansion algorithm [16], the computational time depends on the graph size and number of labels. Since the velocity field (our labels) is composed of real valued 2D vectors, a direct application of [16] is extremely time consuming. We propose a locally adaptive algorithm as follows: $d\mathbf{v}_g$ is restricted to integer values (between -5 to +5, for

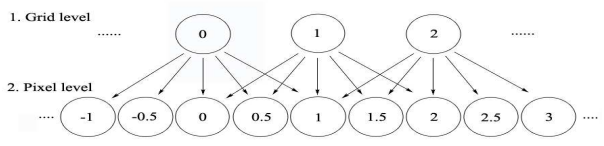

Fig. 1. Illustration of label repartition from grid to pixel level

each component); the number of possible configurations is then kept relatively small. $d\mathbf{v}_l$ is restricted to decimal values (laying within a range from -1 to +1, with a step that fixes the accuracy of the final velocity field) (see figure 1). This digressive approach enables to reduce the computation cost, without affecting the final result.

4. RESULTS

We evaluate the efficiency of our approach on synthetic data and real fluid flow sequences. We use the Average Angle Error (AAE) criteria to compare with results obtained from other methods proposed in the literature [2, 10]:

$$\text{AE} = arccos\left(\frac{\vec{w}_c(s).\vec{w}_e(s)}{||\vec{w}_c(s)||\ ||\vec{w}_e(s)||}\right) \quad (6)$$

AE is the angle between the correct velocity $\vec{w}_c$ and the estimated velocity $\vec{w}_e$, where $\vec{w}_{c,e}(s) = (u_{c,e}(s), v_{c,e}(s), 1)$. As in [2], we pre-process the data by convolving each frame of the sequence with a smoothing Gaussian filter ($\sigma = 0.5$).

Yosemite sequence

The Yosemite sequence [2] is processed with our DOF-MM algorithm, using a pyramid level of 3, and a grid size of 5×5 pixels for the computation of $d\mathbf{v}_g$. When computing the AAE value, we take an offset of 10 pixels on the borders of the image, for the sake of comparability. The Yosemite sequence contains large displacements over 4 pixels in between two frames.

Figure 3 illustrates the spatial map of the AE obtained by ICM and Graph-Cuts. In Fig. 3(c) and 3(d), small AE are observed in blue. The AE in lower half of the image is very small. We observe a difference in the smoothness of the velocity error field. It stems from the fact that, for ICM, the regularization term uses a L2 norm, while α-expansion uses a L1 norm [16]. Moreover, Graph-Cut minimization tends to estimate regular zones of identical label, due to a strong regularization (no time dependent weight) and a limited number of labels; note that if one attenuates the regularization factor, the error rate increases. In our experiments, minimization with Graph-Cuts takes about 3 more times than with ICM.

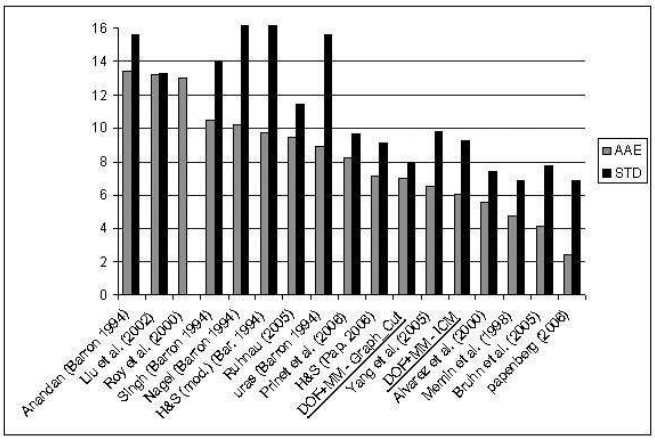

Fig. 2. Algorithm result's comparison on Yosemite. AAE: Average Angle Error; STD: Standard Deviation (degree).

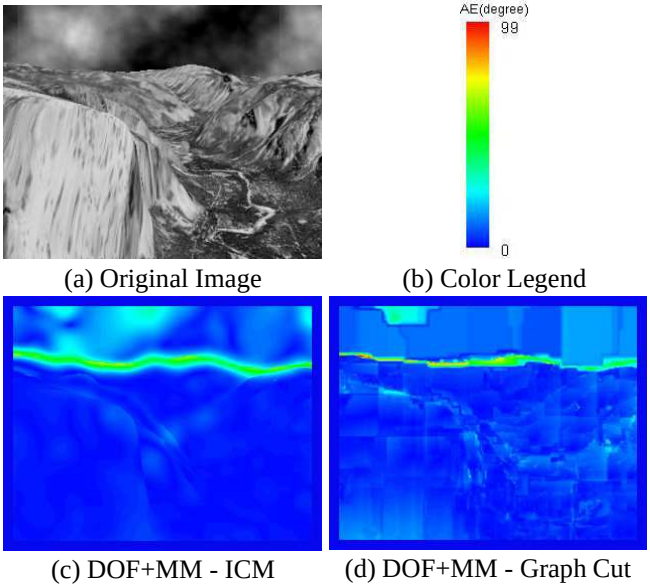

(a) Original Image (b) Color Legend

(c) DOF+MM - ICM (d) DOF+MM - Graph Cut

Fig. 3. Angle Error map for ICM and Graph Cut minimization

Figure 2 gives the AAE and the Standard Deviation (STD) of AE obtained from several optical flow algorithms, ordered from the worst to the best (in term of AAE) from left to right. Our approaches are underlined. Most of the algorithms having a AAE superior to 9 degrees do not integrate multi-resolution techniques. They cannot detect true motion over 1 pixel per frame. All approaches that outperform ours, call for a more sophisticated energy function: they include robust functions [10, 9, 7], or add new assumptions, such as the intensity gradient constancy [11]. Approaches which define an energy function identical to ours (Prinet [14], H&S implemented by Panenberg [11] and Yang [8]) give worse results, both in terms of AAE and STD. Our results from DOF+MM-ICM give lower AAE than from DOF+MM-Graph, but higher STD.

Real fluid flow sequence

The fluid flow sequence that we analyze was acquired in laboratory [17]. The experiment consists of a box filled with water animated with induced movement: a non-homogeneous non-uniform spatial distribution of the temperature in the fluid leads to natural phenomena of convection [17]. Images are acquired in a plane perpendicular to the particle displacement. The average displacement is about 4 pixels per frame, the maximum displacement about 15 pixels per frame.

Figure 4 illustrates the input data and the estimated velocity field computed from Ruhnau algorithm [10] (top right) and from ours (DOF-MM, bottom). Graph-Cut gives poor

results, unable to retrieve correctly large amplitude displacements in non homogeneous regions. Results from DOF-MM-+ICM show that the regularization term tends to oversmooth the velocity field. Visually, DOF-MM+ICM gives results similar to Ruhnau's one. Note that Ruhnau's approach is dedicated to the study of fluid motion, while ours are not; in particular, he integrates specific function to conserve the discontinuities. The simple DOF-based energy function that we use gives very encouraging results, hardly achieved with others algorithmic implementations.

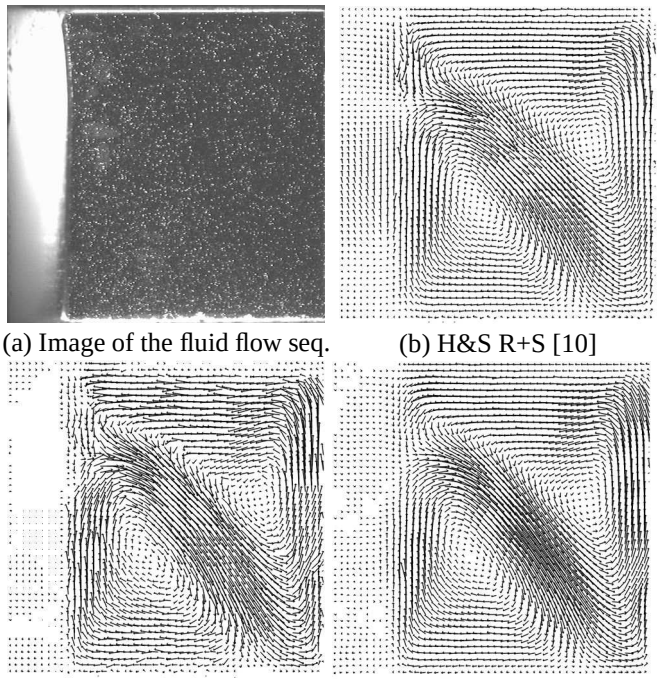

(a) Image of the fluid flow seq. (b) H&S R+S [10]

(d) DOF+MM - Graph Cut (c) DOF+MM - ICM

Fig. 4. Velocity field estimation from a fluid flow sequence.

5. CONCLUSION AND PERSPECTIVES

We introduced a hybrid multi-resolution multi-grid approach to efficiently estimate dense displacement fields between two consecutive frames. Based on the Differential Optical Flow formulation, it estimates large displacement vector field with a significant improvement of the computation time. We compared two energy minimization techniques. We observed empirically (it could not be illustrated in this paper due to space limitation) that the improved ICM always converges to the same minimum (hopefully global minimum). We showed from synthetic and real sequences that our DOF-MM+ICM framework outperforms all existing methods using similar energy function.

However, not only the algorithmic scheme but also the definition of the energy function is crucial for an accurate estimation. The energy function has to be defined according to the chosen application. Further works will focus on fluid motion for the analysis of turbulent flows.

6. REFERENCES

[1] B.K.P. Horn and B.G. Schunck, "Determining optical flow," *Artificial Intelligence*, vol. 17, no. 1-3, pp. 185–203, August 1981.

[2] J.L. Barron, D.J. Fleet, and S.S. Beauchemin, "Performance of optical flow techniques," *IJCV*, vol. 12, no. 1, pp. 43–77, February 1994.

[3] J.R. Bergen, P. Anandan, K.J. Hanna, and R. Hingorani, "Hierarchical model-based motion estimation," in *Proc. ECCV*, 1992, pp. 177–189.

[4] E.P. Simoncelli and W.T. Freeman, "The steerable pyramid: A flexible architecture for multi-scale derivative computation," in *Proc. ICIP*, Washington, DC, USA, October 1995, vol. 3, pp. 444–447.

[5] H. Liu, A. Rosenfeld, and R. Chellapa, "Two-frame multi-scale optical flow estimation using wavelet decomposition," in *Proc. ICASSP*, 2002.

[6] E. Memin and P. Perez, "A multigrid approach to hierarchical motion estimation," in *Proc. ICCV*, 1998, pp. 933–938.

[7] L. Alvarez, J. Weickert, and J. Sanchez, "Reliable estimation of dense optical flow fields with large displacements," *IJCV*, vol. 39, no. 1, pp. 41–56, August 2000.

[8] L. Yang and H. Sahli, "A nonlinear multigrid diffusion model for efficient dense optical flow estimation," in *Pro. ICIP*, September 2005, vol. 1, pp. 149–152.

[9] E. Memin and P. Perez, "Dense estimation and object-based segmentation of the optical-flow with robust techniques," *IEEE on IP*, vol. 7, no. 5, pp. 703–719, May 1998.

[10] P. Ruhnau, T. Kohlberger, H. Nobach, and C. Schnorr, "Variational optical flow estimation for particle image velocimetry," *Exp. in Fluids*, pp. 21–32, 2005.

[11] N. Papenberg, A. Bruhn, T. Brox, S. Didas, and J. Weickert, "Highly accurate optic flow computation with theoretically justified warping," *IJCV*, vol. 67, pp. 141–158, 2006.

[12] S. Roy and V. Govindu, "Mrf solutions for probabilistic optical flow formulations," in *Proc. ICPR*, 2000, vol. 3, pp. 1041–1047.

[13] P.J. Burt and E.H. Adelson, "The laplacian pyramid as a compact image code," *IEEE on Communication*, vol. 31, no. 4, pp. 532–540, 1983.

[14] V. Prinet, C. Cassisa, and F.F. Tang, "Mrf modeling for optical flow computation for multi-structure objects," in *Proc. ICIP*, 2006.

[15] J. Besag, "The statistical analysis of dirty pictures," *J. of the Royal Society*, vol. 48, no. 3, pp. 259–302, 1986.

[16] Y. Boykov and V. Kolmogorov, "An experimental comparison of min-cut/max-flow algorithms for energy minimization in vision," *IEEE on PAMI*, pp. 1124–1137, 2004.

[17] G.M. Quenot, J. Pakleza, and T.A. Kowalewski, "Piv with optical flow," *Exp. in Fluids*, pp. 177–189, 1998.

[18] D. Bereziat, I. Herlin, and L. Younes, "Motion estimation using a volume conservation hypothesis," in *Proc. ICASSP*, March 1999, pp. 3385–3388, Phoenix.

[19] L.K. Su and W.J.A. Dahm, "Scalar imaging velocimetry measurements of the velocity gradient tensor field in turbulent flows. i. assessment of errors," *Phys. of Fluid*, vol. 8, pp. 1869–1882, 1996.

[20] J. Weickert and C. Schnorr, "Variational optic flow computation with a spatio-temporal smoothness constraint," *JMIV*, vol. 14, no. 3, pp. 245–255, May 2001.

[21] T. Corpetti, E. Memin, and P. Perez, "Dense estimation of fluid flow," *IEEE on PAMI*, pp. 365–380, 2002.